

A SCALE INVARIANT APPROACH FOR SPARSE SIGNAL RECOVERY*

YAGHOUB RAHIMI[†], CHAO WANG^{†‡}, HONGBO DONG[§], AND YIFEI LOU[†]

Abstract. In this paper, we study the ratio of the L_1 and L_2 norms, denoted as L_1/L_2 , to promote sparsity. Due to the non-convexity and non-linearity, there has been little attention to this scale-invariant model. Compared to popular models in the literature such as the L_p model for $p \in (0, 1)$ and the transformed L_1 (TL1), this ratio model is parameter free. Theoretically, we present a strong null space property (sNSP) and prove that any sparse vector is a local minimizer of the L_1/L_2 model provided with this sNSP condition. Computationally, we focus on a constrained formulation that can be solved via the alternating direction method of multipliers (ADMM). Experiments show that the proposed approach is comparable to the state-of-the-art methods in sparse recovery. In addition, a variant of the L_1/L_2 model to apply on the gradient is also discussed with a proof-of-concept example of the MRI reconstruction.

Key words. Sparsity, L_0 , L_1 , null space property, alternating direction method of multipliers, MRI reconstruction

AMS subject classifications. 90C90, 65K10, 49N45, 49M20

1. Introduction. Sparse signal recovery is to find the sparsest solution of $A\mathbf{x} = \mathbf{b}$ where $\mathbf{x} \in \mathbb{R}^n$, $\mathbf{b} \in \mathbb{R}^m$, and $A \in \mathbb{R}^{m \times n}$ for $m \ll n$. This problem is often referred to as *compressed sensing* (CS) in the sense that the sparse signal \mathbf{x} is compressible. Mathematically, this fundamental problem in CS can be formulated as

$$(1.1) \quad \min_{\mathbf{x} \in \mathbb{R}^n} \|\mathbf{x}\|_0 \quad \text{s.t.} \quad A\mathbf{x} = \mathbf{b},$$

where $\|\mathbf{x}\|_0$ is the number of nonzero entries in \mathbf{x} . Unfortunately, (1.1) is NP-hard [31] to solve. A popular approach in CS is to replace L_0 by the convex L_1 norm, i.e.,

$$(1.2) \quad \min_{\mathbf{x} \in \mathbb{R}^n} \|\mathbf{x}\|_1 \quad \text{s.t.} \quad A\mathbf{x} = \mathbf{b}.$$

Computationally, there are various L_1 minimization algorithms such as primal dual [8], forward-backward splitting [34], and alternating direction method of multipliers (ADMM) [4].

A major breakthrough in CS was the *restricted isometry property* (RIP) [6], which provides a sufficient condition of minimizing the L_1 norm to recover the sparse signal. There is a necessary and sufficient condition given in terms of null space of the matrix A , thus referred to as *null space property* (NSP); see Definition 1.1.

DEFINITION 1.1 (null space property [10]). *For any matrix $A \in \mathbb{R}^{m \times n}$, we say the matrix A satisfies a null space property (NSP) of order s if*

$$(1.3) \quad \|\mathbf{v}_S\|_1 < \|\mathbf{v}_{S^c}\|_1, \quad \mathbf{v} \in \ker(A) \setminus \{\mathbf{0}\}, \quad \forall S \subset [n], \quad |S| \leq s,$$

*Submitted to the journal's Methods and Algorithms for Scientific Computing section December 18, 2018.

Funding: YR and YL were partially supported by NSF grants DMS-1522786 and CAREER 1846690.

[†]Department of Mathematical Sciences, University of Texas at Dallas, Richardson, TX 75080 (yxr160430@utdallas.edu, chaowang.hk@gmail.com, yifei.lou@utdallas.edu).

[‡]the corresponding author.

[§]Department of Mathematics and Statistics, Washington State University, Pullman, WA 99164 (hongbo.dong@wsu.edu).

where $[n] := \{1, \dots, n\}$, \bar{S} is the complement of S , i.e., $[n] \setminus S$, and \mathbf{x}_S is defined as

$$(\mathbf{x}_S)_i = \begin{cases} x_i & \text{if } i \in S, \\ 0 & \text{otherwise.} \end{cases}$$

The null space of A is denoted by $\ker(A) := \{\mathbf{x} \mid A\mathbf{x} = \mathbf{0}\}$.

Donoho and Huo [12] proved that every s -sparse signal $\mathbf{x} \in \mathbb{R}^n$ is the unique solution to the L_1 minimization (1.2) if and only if A satisfies the NSP of order s . NSP quantifies the notion that vectors in the null space of A should not be too concentrated on a small subset of indices. Since it is a necessary and sufficient condition, NSP is widely used in proving other exact recovery guarantees. Note that NSP is no longer necessary if “every s -sparse vector” is relaxed. A weaker¹ sufficient condition for the exact L_1 recovery was proved by Zhang [49]. It is stated that if a vector \mathbf{x}^* satisfies $A\mathbf{x}^* = \mathbf{b}$ and

$$(1.4) \quad \sqrt{\|\mathbf{x}^*\|_0} < \frac{1}{2} \min_{\mathbf{v}} \left\{ \frac{\|\mathbf{v}\|_1}{\|\mathbf{v}\|_2} : \mathbf{v} \in \ker(A) \setminus \{\mathbf{0}\} \right\},$$

then \mathbf{x}^* is the unique solution to both (1.1) and (1.2). Unfortunately, neither RIP nor NSP can be numerically verified for a given matrix [1, 38].

Alternatively, a computable condition for L_1 's exact recovery is based on *coherence*, which is defined as

$$(1.5) \quad \mu(A) := \max_{i \neq j} \frac{|\mathbf{a}_i^T \mathbf{a}_j|}{\|\mathbf{a}_i\| \|\mathbf{a}_j\|},$$

for a matrix $A = [\mathbf{a}_1, \dots, \mathbf{a}_N]$. Donoho-Elad [11] and Gribonval [16] proved independently that if \mathbf{x}^* satisfies $A\mathbf{x}^* = \mathbf{b}$ and

$$(1.6) \quad \|\mathbf{x}^*\|_0 < \frac{1}{2} \left(1 + \frac{2}{\mu(A)} \right),$$

then \mathbf{x}^* is the optimal solution to both (1.1) and (1.2). Clearly, the coherence $\mu(A)$ is bounded by $[0, 1]$. The inequality (1.6) implies that L_1 may not perform well for highly coherent matrices, i.e., $\mu(A) \sim 1$, as $\|\mathbf{x}\|_0$ is then at most one, which seldom occurs simultaneously with $A\mathbf{x}^* = \mathbf{b}$.

Other than the popular L_1 norm, there are a variety of regularization functionals to promote sparsity, such as L_p [9, 43, 23], L_1 - L_2 [44, 26], capped L_1 (CL1) [48, 37], and transformed L_1 (TL1) [29, 46, 47]. Most of these models are nonconvex, leading to difficulties in proving exact recovery guarantees and algorithmic convergence, but they tend to give better empirical results compared to the convex L_1 approach. For example, it was reported in [44, 26] that L_p gives superior results for incoherent matrices (i.e., $\mu(A)$ is small), while L_1 - L_2 is the best for the coherent scenario. In addition, TL1 is always the second best no matter whether the matrix is coherent or not [46, 47].

In this paper, we study the ratio of L_1 and L_2 as a scale-invariant model to approximate the desired L_0 , which is scale-invariant itself. In one dimensional (1D) case (i.e., $n = 1$), the L_1/L_2 model is exactly the same as the L_0 model if we use the convention $\frac{0}{0} = 0$. The ratio of L_1 and L_2 was first proposed by Hoyer [20] as a sparseness measure and later highlighted in [21] as a scale-invariant model. However, there has been little attention on it due to its computational difficulties arisen

¹The sufficient condition of (1.4) is weaker than the one in (1.3).

from being non-convex and non-linear. There are some theorems that establish the equivalence between the L_1/L_2 and the L_0 models, but only restricted to nonnegative signals [13, 44]. We aim to apply this ratio model to arbitrary signals. On the other hand, the L_1/L_2 minimization has an intrinsic drawback that it tends to produce one erroneously large coefficient while suppressing the other non-zero elements, under which case the ratio is reduced. To compensate for this drawback, it is helpful to incorporate a box constraint, which will also be addressed in this paper.

Now we turn to a sparsity-related assumption that signal is sparse after a given transform, as opposed to signal itself being sparse. This assumption is widely used in image processing. For example, a natural image, denoted by u , is mostly sparse after taking gradient, and hence it is reasonable to minimize the L_0 norm of the gradient, i.e., $\|\nabla u\|_0$. To bypass the NP-hard L_0 norm, the convex relaxation replaces L_0 by L_1 , where the L_1 norm of the gradient is the well-known total variation (TV) [36] of an image. A weighted L_1 - αL_2 model (for $\alpha > 0$) on the gradient was proposed in [27], which suggested that $\alpha = 0.5$ yields better results than $\alpha = 1$ for image denoising, deblurring, and MRI reconstruction. The ratio of L_1 and L_2 on the image gradient was used in deconvolution and blind deconvolution [22, 35]. We further adapt the proposed ratio model from sparse signal recovery to imaging applications, specifically focusing on MRI reconstruction.

The rest of the paper is organized as follows. Section 2 is devoted to theoretical analysis of the L_1/L_2 model. In Section 3, we apply the ADMM to minimize the ratio of L_1 and L_2 with two variants of incorporating a box constraint as well as applying on the image gradient. We conduct extensive experiments in Section 4 to demonstrate the performance of the proposed approaches over the state-of-the-art in sparse recovery and MRI reconstruction. Section 5 is a fun exercise, where we use the L_1/L_2 minimization to compute the right-hand-side of the NSP condition (1.4), leading to an empirical upper bound of the exact L_1 recovery guarantee. Finally, conclusions and future works are given in Section 6.

2. Rationales of the L_1/L_2 model. We begin with a toy example to illustrate the advantages of L_1/L_2 over other alternatives, followed by some theoretical properties of the proposed model.

2.1. Toy example. Define a matrix A as

$$(2.1) \quad A := \begin{bmatrix} 1 & -1 & 0 & 0 & 0 & 0 \\ 1 & 0 & -1 & 0 & 0 & 0 \\ 0 & 1 & 1 & 1 & 0 & 0 \\ 2 & 2 & 0 & 0 & 1 & 0 \\ 1 & 1 & 0 & 0 & 0 & -1 \end{bmatrix} \in \mathbb{R}^{5 \times 6},$$

and $\mathbf{b} = (0, 0, 20, 40, 18)^T \in \mathbb{R}^5$. It is straightforward that any general solutions of $A\mathbf{x} = \mathbf{b}$ have the form of $\mathbf{x} = (t, t, t, 20 - 2t, 40 - 4t, 2(t - 9))^T$ for a scalar $t \in \mathbb{R}$. The sparsest solution occurs at $t = 0$, where the sparsity of \mathbf{x} is 3 and some local solutions include $t = 10$ for sparsity being 4 and $t = 9$ for sparsity being 5. In Figure 1, we plot various objective functions with respect to t , including L_1, L_p (for $p = 1/2$), L_1 - L_2 , and TL1 (for $a = 1$ as suggested in [47]). Note that all these functions are not differentiable at the values of $t = 0, 9$, and 10, where the sparsity of \mathbf{x} is strictly smaller than 6. The sparsest vector \mathbf{x} corresponding to $t = 0$ can only be found by minimizing TL1 and L_1/L_2 , while the other models find $t = 10$ as a global minimum.

2.2. Theoretical properties. Recently, Tran and Webster [39] generalized the NSP to deal with sparse promoting metrics that are symmetric, separable and concave, which unfortunately does not apply to L_1/L_2 (not separable), but this work motivates us to consider a stronger form of the NSP, as defined in Definition 2.1.

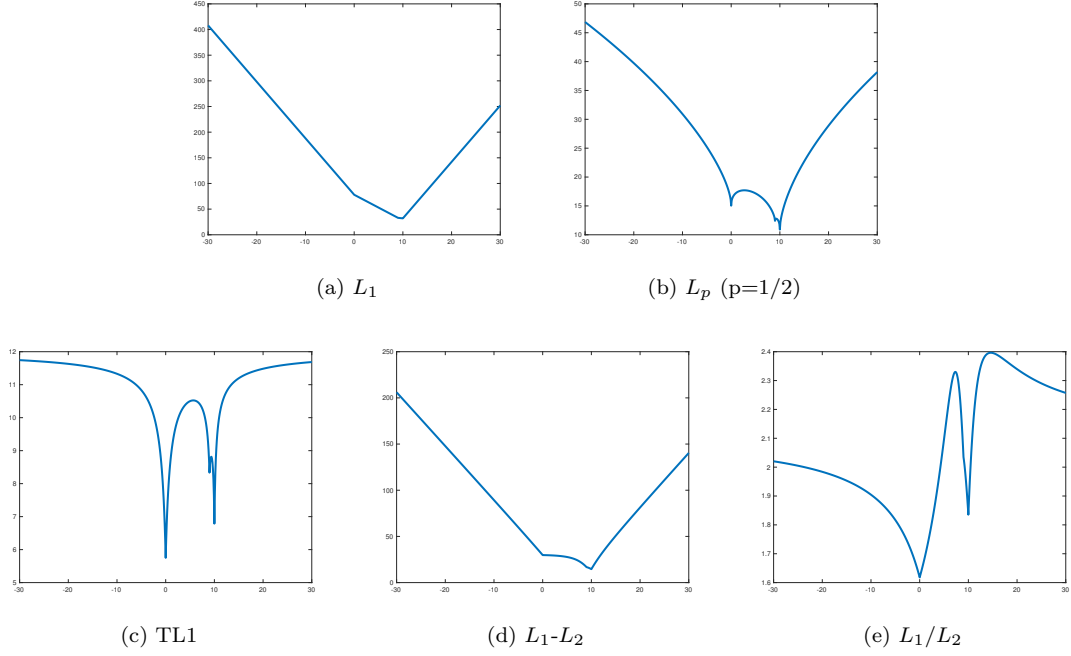


FIG. 1. The objective functions of a toy example illustrate that only L_1/L_2 and TL1 can find $t = 0$ as the global minimizer, but TL1 has a very narrow basin of attraction (thus sensitive to initial guess and difficult to find the global solution.).

DEFINITION 2.1. For any matrix $A \in \mathbb{R}^{m \times n}$, we say the matrix A satisfies a strong null space property (sNSP) of order s if

$$(2.2) \quad (s+1) \|\mathbf{v}_S\|_1 \leq \|\mathbf{v}_{\bar{S}}\|_1, \quad \mathbf{v} \in \ker(A) \setminus \{\mathbf{0}\}, \quad \forall S \subset [n], \quad |S| \leq s.$$

Note that Definition 2.1 is stronger than the original NSP in Definition 1.1 in the sense that if a matrix satisfies sNSP then it also satisfies the original NSP. The following theorem says that any s -sparse vector is a local minimizer of L_1/L_2 provided the matrix has the sNSP of order s . The proof is given in Appendix.

THEOREM 2.2. Assume an $m \times n$ matrix A satisfies the sNSP of order s , then any s -sparse solution of $A\mathbf{x} = \mathbf{b}$ ($\mathbf{b} \neq \mathbf{0}$) is a local minimum for L_1/L_2 in the feasible space of $A\mathbf{x} = \mathbf{b}$. i.e., there exists a positive number $t^* > 0$ such that for every $\mathbf{v} \in \ker(A)$ with $0 < \|\mathbf{v}\|_2 \leq t^*$ we have

$$(2.3) \quad \frac{\|\mathbf{x}\|_1}{\|\mathbf{x}\|_2} \leq \frac{\|\mathbf{x} + \mathbf{v}\|_1}{\|\mathbf{x} + \mathbf{v}\|_2}.$$

Finally, we show the optimal value of the L_1/L_2 subject to $A\mathbf{x} = \mathbf{b}$ is upper bounded by the same ratio with $\mathbf{b} = \mathbf{0}$; see Proposition 1.

PROPOSITION 1. For any $A \in \mathbb{R}^{m \times n}$, $\mathbf{x} \in \mathbb{R}^n$, we have

$$(2.4) \quad \inf_{\mathbf{z} \in \mathbb{R}^n} \left\{ \frac{\|\mathbf{z}\|_1}{\|\mathbf{z}\|_2} \mid A\mathbf{z} = A\mathbf{x} \right\} \leq \inf_{\mathbf{z} \in \mathbb{R}^n} \left\{ \frac{\|\mathbf{z}\|_1}{\|\mathbf{z}\|_2} \mid \mathbf{z} \in \ker(A) \setminus \{\mathbf{0}\} \right\}.$$

Proof. Denote

$$(2.5) \quad \alpha^* = \inf_{\mathbf{z} \in \mathbb{R}^n} \left\{ \frac{\|\mathbf{z}\|_1}{\|\mathbf{z}\|_2} \mid A\mathbf{z} = A\mathbf{x} \right\}.$$

For every $\mathbf{v} \in \ker(A) \setminus \{\mathbf{0}\}$ and $t \in \mathbb{R}$, we have that

$$(2.6) \quad \alpha^* \leq \frac{\|\mathbf{x} + t\mathbf{v}\|_1}{\|\mathbf{x} + t\mathbf{v}\|_2},$$

since $A(\mathbf{x} + t\mathbf{v}) = \mathbf{b}$. Then we obtain

$$(2.7) \quad \lim_{t \rightarrow \infty} \frac{\|\mathbf{x} + t\mathbf{v}\|_1}{\|\mathbf{x} + t\mathbf{v}\|_2} = \lim_{t \rightarrow \infty} \frac{\|\mathbf{x}/t + \mathbf{v}\|_1}{\|\mathbf{x}/t + \mathbf{v}\|_2} = \frac{\|\mathbf{v}\|_1}{\|\mathbf{v}\|_2}.$$

Therefore, for every $\mathbf{v} \in \ker(A) \setminus \{\mathbf{0}\}$,

$$(2.8) \quad \alpha^* \leq \frac{\|\mathbf{v}\|_1}{\|\mathbf{v}\|_2},$$

which directly leads to the desired inequality (2.4). \square

Proposition 1 implies that the left-hand-side of the inequality involves both the underlying signal \mathbf{x} and the system matrix A , which can be upper bounded by the minimum ratio that only involves A .

3. Numerical schemes. The proposed model is

$$(3.1) \quad \min_{\mathbf{x} \in \mathbb{R}^n} \left\{ \frac{\|\mathbf{x}\|_1}{\|\mathbf{x}\|_2} + I_0(A\mathbf{x} - \mathbf{b}) \right\},$$

where $I_S(\mathbf{t})$ is the function enforcing \mathbf{t} into the feasible set S , i.e.,

$$(3.2) \quad I_S(\mathbf{t}) = \begin{cases} 0 & \mathbf{t} \in S, \\ +\infty & \text{otherwise.} \end{cases}$$

In [Subsection 3.1](#), we detail the ADMM algorithm for minimizing (3.1), followed by a minor change to incorporate additional box constraint in [Subsection 3.2](#). We discuss in [Subsection 3.3](#) another variant of L_1/L_2 on the gradient to deal with imaging applications.

3.1. The L_1/L_2 minimization via ADMM. In order to apply the ADMM [4] to solve for (3.1), we introduce two auxiliary variables and rewrite (3.1) into an equivalent form,

$$(3.3) \quad \min_{\mathbf{x}, \mathbf{y}, \mathbf{z}} \left\{ \frac{\|\mathbf{z}\|_1}{\|\mathbf{y}\|_2} + I_0(A\mathbf{x} - \mathbf{b}) \right\} \quad \text{s.t.} \quad \mathbf{x} = \mathbf{y}, \quad \mathbf{x} = \mathbf{z}.$$

The augmented Lagrangian for (3.3) is

$$(3.4) \quad \begin{aligned} L_{\rho_1, \rho_2}(\mathbf{x}, \mathbf{y}, \mathbf{z}; \mathbf{v}, \mathbf{w}) &= \frac{\|\mathbf{z}\|_1}{\|\mathbf{y}\|_2} + I_0(A\mathbf{x} - \mathbf{b}) + \langle \mathbf{v}, \mathbf{x} - \mathbf{y} \rangle + \frac{\rho_1}{2} \|\mathbf{x} - \mathbf{y}\|_2^2 + \langle \mathbf{w}, \mathbf{x} - \mathbf{z} \rangle + \frac{\rho_2}{2} \|\mathbf{x} - \mathbf{z}\|_2^2 \\ &= \frac{\|\mathbf{z}\|_1}{\|\mathbf{y}\|_2} + I_0(A\mathbf{x} - \mathbf{b}) + \frac{\rho_1}{2} \left\| \mathbf{x} - \mathbf{y} + \frac{1}{\rho_1} \mathbf{v} \right\|_2^2 + \frac{\rho_2}{2} \left\| \mathbf{x} - \mathbf{z} + \frac{1}{\rho_2} \mathbf{w} \right\|_2^2. \end{aligned}$$

The ADMM consists of the following five steps:

$$(3.5) \quad \begin{cases} \mathbf{x}^{(k+1)} := \arg \min_{\mathbf{x}} L_{\rho_1, \rho_2}(\mathbf{x}, \mathbf{y}^{(k)}, \mathbf{z}^{(k)}; \mathbf{v}^{(k)}, \mathbf{w}^{(k)}), \\ \mathbf{y}^{(k+1)} := \arg \min_{\mathbf{y}} L_{\rho_1, \rho_2}(\mathbf{x}^{(k+1)}, \mathbf{y}, \mathbf{z}^{(k)}; \mathbf{v}^{(k)}, \mathbf{w}^{(k)}), \\ \mathbf{z}^{(k+1)} := \arg \min_{\mathbf{z}} L_{\rho_1, \rho_2}(\mathbf{x}^{(k+1)}, \mathbf{y}^{(k+1)}, \mathbf{z}; \mathbf{v}^{(k)}, \mathbf{w}^{(k)}), \\ \mathbf{v}^{(k+1)} := \mathbf{v}^{(k)} + \rho_1(\mathbf{x}^{(k+1)} - \mathbf{y}^{(k+1)}), \\ \mathbf{w}^{(k+1)} := \mathbf{w}^{(k)} + \rho_2(\mathbf{x}^{(k+1)} - \mathbf{z}^{(k+1)}). \end{cases}$$

The update for \mathbf{x} is a projection to the affine space of $A\mathbf{x} = \mathbf{b}$,

$$\begin{aligned} \mathbf{x}^{(k+1)} &:= \arg \min_{\mathbf{x}} L_{\rho_1, \rho_2}(\mathbf{x}, \mathbf{y}^{(k)}, \mathbf{z}^{(k)}; \mathbf{v}^{(k)}, \mathbf{w}^{(k)}) \\ &= \arg \min_{\mathbf{x}} \left\{ \frac{\rho_1 + \rho_2}{2} \|\mathbf{x} - \mathbf{f}^{(k)}\|_2^2 \text{ s.t. } A\mathbf{x} = \mathbf{b} \right\} \\ &= (I - A^T(AA^T)^{-1}A) \mathbf{f}^{(k)} + A^T(AA^T)^{-1}\mathbf{b}, \end{aligned}$$

where

$$(3.6) \quad \mathbf{f}^{(k)} = \frac{\rho_1}{\rho_1 + \rho_2} \left(\mathbf{y}^{(k)} - \frac{1}{\rho_1} \mathbf{v}^{(k)} \right) + \frac{\rho_2}{\rho_1 + \rho_2} \left(\mathbf{z}^{(k)} - \frac{1}{\rho_2} \mathbf{w}^{(k)} \right).$$

As for the \mathbf{y} -subproblem, let $c^{(k)} = \|\mathbf{z}^{(k)}\|_1$ and $\mathbf{d}^{(k)} = \mathbf{x}^{(k+1)} + \frac{\mathbf{v}^{(k)}}{\rho_1}$ and the minimization subproblem reduces to

$$(3.7) \quad \mathbf{y}^{(k+1)} = \arg \min_{\mathbf{y}} \frac{c^{(k)}}{\|\mathbf{y}\|_2} + \frac{\rho_1}{2} \|\mathbf{y} - \mathbf{d}^{(k)}\|_2^2.$$

If $\mathbf{d}^{(k)} = 0$ then any vector \mathbf{y} with $\|\mathbf{y}\|_2 = \sqrt[3]{\frac{c^{(k)}}{\rho_1}}$ is a solution to the minimization problem. If $c^{(k)} = 0$ then $\mathbf{y} = \mathbf{d}^{(k)}$ is the solution. Now we consider $\mathbf{d}^{(k)} \neq 0$ and $c^{(k)} \neq 0$. By taking derivative of the objective function with respect to \mathbf{y} , we obtain

$$\left(-\frac{c^{(k)}}{\|\mathbf{y}\|_2^3} + \rho_1 \right) \mathbf{y} = \rho_1 \mathbf{d}^{(k)}.$$

As a result, there exists a positive number $\tau^{(k)} \geq 0$ such that $\mathbf{y} = \tau^{(k)} \mathbf{d}^{(k)}$. Given $\mathbf{d}^{(k)}$, we denote $\eta^{(k)} = \|\mathbf{d}^{(k)}\|_2$. For $\eta^{(k)} > 0$, finding \mathbf{y} becomes a one-dimensional search for the parameter $\tau^{(k)}$. In other words, if we take $D^{(k)} = \frac{c^{(k)}}{\rho_1(\eta^{(k)})^3}$, then $\tau^{(k)}$ is a root of

$$\underbrace{\tau^3 - \tau^2 - D^{(k)}}_{F(\tau)} = 0.$$

The cubic-root formula suggests that $F(\tau) = 0$ has only one real root, which can be found by the following closed-form solution.

$$(3.8) \quad \tau^{(k)} = \frac{1}{3} + \frac{1}{3} \left(C^{(k)} + \frac{1}{C^{(k)}} \right), \text{ with } C^{(k)} = \sqrt[3]{\frac{27D^{(k)} + 2 + \sqrt{(27D^{(k)} + 2)^2 - 4}}{2}}.$$

In summary, we have

$$(3.9) \quad \mathbf{y}^{(k+1)} = \begin{cases} \mathbf{e}^{(k)} & \mathbf{d}^{(k)} = 0, \\ \tau^{(k)} \mathbf{d}^{(k)} & \mathbf{d}^{(k)} \neq 0, \end{cases}$$

where $\mathbf{e}^{(k)}$ is a random vector with the L_2 norm to be $\sqrt[3]{\frac{c^{(k)}}{\rho_1}}$.

Finally, the ADMM update for \mathbf{z} is

$$(3.10) \quad \mathbf{z}^{(k+1)} = \mathbf{shrink} \left(\mathbf{x}^{(k+1)} + \frac{\mathbf{w}^{(k)}}{\rho_2}, \frac{1}{\rho_2 \|\mathbf{y}^{(k+1)}\|_2} \right),$$

where **shrink** is often referred to as *soft shrinkage* operator,

$$(3.11) \quad \mathbf{shrink}(\mathbf{v}, \mu)_i = \text{sign}(v_i) \max(|v_i| - \mu, 0), \quad i = 1, 2, \dots, n.$$

We summarize the ADMM algorithm for solving the L_1/L_2 minimization problem in [Algorithm 3.1](#).

Algorithm 3.1 The L_1/L_2 minimization via ADMM.

Input: $A \in \mathbb{R}^{m \times n}$, $\mathbf{b} \in \mathbb{R}^{m \times 1}$, Max and $\epsilon \in \mathbb{R}$
while $k < \text{Max}$ or $\|\mathbf{x}^{(k)} - \mathbf{x}^{(k-1)}\|_2 / \|\mathbf{x}^{(k)}\| > \epsilon$ **do**
 $\mathbf{x}^{(k+1)} = (I - A^T(AA^T)^{-1}A) \mathbf{f}^{(k)} + A^T(AA^T)^{-1}\mathbf{b}$
 $\mathbf{y}^{(k+1)} = \begin{cases} \mathbf{e}^{(k)} & \mathbf{d}^{(k)} = 0 \\ \tau^{(k)} \mathbf{d}^{(k)} & \mathbf{d}^{(k)} \neq 0 \end{cases}$
 $\mathbf{z}^{(k+1)} = \mathbf{shrink} \left(\mathbf{x}^{(k+1)} + \frac{\mathbf{w}^{(k)}}{\rho_2}, \frac{1}{\rho_2 \|\mathbf{y}^{(k+1)}\|_2} \right)$
 $\mathbf{v}^{(k+1)} = \mathbf{v}^{(k)} + \rho_1(\mathbf{x}^{(k+1)} - \mathbf{y}^{(k+1)})$
 $\mathbf{w}^{(k+1)} = \mathbf{w}^{(k)} + \rho_2(\mathbf{x}^{(k+1)} - \mathbf{z}^{(k+1)})$
 $k = k+1$
end while
return $\mathbf{x}^{(k)}$

REMARK 1. We can pre-compute the matrix $I - A^T(AA^T)^{-1}A$ and the vector $A^T(AA^T)^{-1}\mathbf{b}$ in [Algorithm 3.1](#). The complexity is $O(m^2n)$ for the pre-computation including the matrix-matrix multiplication and Cholesky decomposition for solving linear system. In each iteration, we need to do matrix-vector multiplication for the \mathbf{x} -subproblem, which is in the order of $O(n^2)$. In the \mathbf{y} -subproblem, the rooting finding is one-dimensional search, whose cost can be neglected. The \mathbf{z} -subproblem is pixel-wise shrinkage operation and only takes $O(n)$. In summary, the computation complexity for each iteration is $O(n^2)$. We can consider the parallel computing to further speed up, thanks to the separation of the \mathbf{z} -subproblem.

3.2. L_1/L_2 with box constraint. The L_1/L_2 model has an intrinsic drawback that tends to produce one erroneously large coefficient while suppressing the other non-zero elements, under which case the ratio is reduced. To compensate for this drawback, it is helpful to incorporate a box constraint, if we know lower/upper bounds of the underlying signal *a priori*. Specifically, we propose

$$(3.12) \quad \min_{\mathbf{x} \in \mathbb{R}^n} \left\{ \frac{\|\mathbf{x}\|_1}{\|\mathbf{x}\|_2} + I_0(A\mathbf{x} - \mathbf{b}) \mid \mathbf{x} \in [c, d] \right\},$$

which is referred to as L_1/L_2 -box. Similar to (3.3), we look at the following form that enforces the box constraint on variable \mathbf{z} ,

$$(3.13) \quad \min_{\mathbf{x}, \mathbf{y}, \mathbf{z}} \left\{ \frac{\|\mathbf{z}\|_1}{\|\mathbf{y}\|_2} + I_0(A\mathbf{x} - \mathbf{b}) \right\} \quad \text{s.t. } \mathbf{x} = \mathbf{y}, \quad \mathbf{x} = \mathbf{z}, \quad \mathbf{z} \in [c, d].$$

The only change we need to make by adapting Algorithm 3.1 to the L_1/L_2 -box is the \mathbf{z} update. The \mathbf{z} -subproblem in (3.5) with the box constraint is

$$(3.14) \quad \min_{\mathbf{z}} \frac{1}{\|\mathbf{y}^{(k+1)}\|_2} \|\mathbf{z}\|_1 + \frac{\rho_2}{2} \|\mathbf{x}^{(k+1)} - \mathbf{z} + \frac{1}{\rho_2} \mathbf{w}^{(k)}\|_2^2 \quad \text{s.t. } \mathbf{z} \in [c, d].$$

For a convex problem (3.14) involving the L_1 norm, it has a closed-form solution given by the soft shrinkage, followed by projection to the interval $[c, d]$. In particular, simple calculations show that

$$(3.15) \quad z_i^{(k+1)} = \min \{ \max(\hat{z}_i, c), d \}, \quad i = 1, 2, \dots, n,$$

where $\hat{\mathbf{z}} = \mathbf{shrink}(\mathbf{r}, \nu)$, $\mathbf{r} = \mathbf{x}^{(k+1)} + \frac{\mathbf{w}^{(k)}}{\rho_2}$ and $\nu = \frac{1}{\rho_2 \|\mathbf{y}^{(k+1)}\|}$. If the box constraint $[c, d]$ is symmetric, i.e., $c = -d$ and $d > 0$, it follows from [2] that the update for \mathbf{z} can be expressed as

$$(3.16) \quad z_i^{(k+1)} = \text{sign}(v_i) \min \{ \max(|r_i| - \nu, 0), d \}, \quad i = 1, 2, \dots, n.$$

REMARK 2. *The existing literature on the ADMM convergence [17, 19, 24, 33, 40, 41, 42] requires the existence of one separable function in the objective function, whose gradient is Lipschitz continuous. Obviously, L_1/L_2 does not satisfy this assumption, no matter with or without the box constraint. Therefore, we have difficulties in analyzing the convergence theoretically. Instead, we show the convergence empirically in Section 4 by plotting residual errors and objective functions, which gives strong supports for theoretical analysis in the future.*

3.3. L_1/L_2 on the gradient. We adapt the L_1/L_2 model to apply on the gradient, which enables us to deal with imaging applications. Let $u \in \mathbb{R}^{n \times m}$ be an underlying image of size $n \times m$. Denote A as a linear operator that models a certain degradation process to obtain the measured data f . For example, A can be a subsampling operator in the frequency domain and recovering u from f is called MRI reconstruction. In short, the proposed gradient model is given by

$$(3.17) \quad \min_{u \in \mathbb{R}^{n \times m}} \frac{\|\nabla u\|_1}{\|\nabla u\|_2} \quad \text{s.t. } Au = f, \quad u \in [0, 1],$$

where ∇ denotes discrete gradient operator $\nabla u := \{[u_{ij} - u_{(i+1)j}]_{i=1}^n\}_{j=1}^m, \{[u_{ij} - u_{i(j+1)}]_{j=1}^m\}_{i=1}^n$ with periodic boundary condition; hence the model is referred to as L_1/L_2 -grad. Note that the box constraint $0 \leq u \leq 1$ is a reasonable assumption in the MRI reconstruction problem.

To solve for (3.17), we introduce three auxiliary variables \mathbf{d} , \mathbf{h} , and v , leading to an equivalent problem,

$$(3.18) \quad \min_{u \in \mathbb{R}^{n \times m}} \frac{\|\mathbf{d}\|_1}{\|\mathbf{h}\|_2} \quad \text{s.t. } Au = f, \quad \mathbf{d} = \nabla u, \quad \mathbf{h} = \nabla u, \quad u = v, \quad 0 \leq v \leq 1.$$

Note that we denote \mathbf{d} and \mathbf{h} in bold to indicate that they have two components corresponding to both x and y derivatives. The augmented Lagrangian is expressed as

$$(3.19) \quad \begin{aligned} \mathcal{L}(u, \mathbf{d}, \mathbf{h}, v; w, \mathbf{b}_1, \mathbf{b}_2, e) &= \frac{\|\mathbf{d}\|_1}{\|\mathbf{h}\|_2} + \frac{\lambda}{2} \|Au - f - w\|_2^2 + \frac{\rho_1}{2} \|\mathbf{d} - \nabla u - \mathbf{b}_1\|_2^2 \\ &\quad + \frac{\rho_2}{2} \|\mathbf{h} - \nabla u - \mathbf{b}_2\|_2^2 + \frac{\rho_3}{2} \|v - u - e\|_2^2 + I_{[0,1]}(v), \end{aligned}$$

where $w, \mathbf{b}_1, \mathbf{b}_2, e$ are dual variables and $\lambda, \rho_1, \rho_2, \rho_3$ are positive parameters. The updates for \mathbf{d}, \mathbf{h} are the same as Algorithm 3.1. Specifically for \mathbf{h} , we consider $D^{(k)} = \frac{\|\mathbf{d}\|_1}{\rho_2 \|\nabla u^{(k+1)} + \mathbf{g}^{(k)}\|_2^3}$ and hence $\tau^{(k)}$ is the root of the same polynomial as in (3.8). By taking derivative of (3.19) with respect to u , we can obtain the u -update, i.e.,

$$(3.20) \quad \begin{aligned} u^{(k+1)} = & (\lambda A^T A - (\rho_1 + \rho_2)\Delta + \rho_3 I)^{-1} \left(\lambda A^T (f + w^{(k)}) \right. \\ & \left. + \rho_1 \nabla^T (\mathbf{d}^{(k)} - \mathbf{b}_1^{(k)}) + \rho_2 \nabla^T (\mathbf{h}^{(k)} - \mathbf{b}_2^{(k)}) + \rho_3 (v^{(k)} - e^{(k)}) \right). \end{aligned}$$

Note for certain operator A , the inverse in the u -update (3.20) can be computed efficiently via the fast Fourier transform (FFT). The v -subproblem is a projection to an interval $[0, 1]$, i.e.,

$$(3.21) \quad v_{ij}^{(k+1)} = \min \left\{ \max(u_{ij}^{(k+1)} + e_{ij}^{(k)}, 0), 1 \right\}, \quad i = 1, 2, \dots, n, j = 1, 2, \dots, m.$$

In summary, we present the ADMM algorithm for the L_1/L_2 -grad model in Algorithm 3.2.

Algorithm 3.2 The L_1/L_2 -grad minimization via ADMM.

Input: $f \in \mathbb{R}^{n \times m}$, A , Max and $\epsilon \in \mathbb{R}$.

while $k < \text{Max}$ or $\|u^{(k)} - u^{(k-1)}\|_2 / \|u^{(k)}\| > \epsilon$ **do**

Solve $u^{(k+1)}$ via (3.20)

Solve $v^{(k+1)}$ via (3.21)

$$\mathbf{h}^{(k+1)} = \begin{cases} \mathbf{e}^{(k)} & \nabla u^{(k+1)} + \mathbf{g}^{(k)} = 0, \\ \tau^{(k)} (\nabla u^{(k+1)} + \mathbf{g}^{(k)}) & \nabla u^{(k+1)} + \mathbf{g}^{(k)} \neq 0. \end{cases}$$

$$\mathbf{d}^{(k+1)} = \text{shrink} \left(\nabla u^{(k+1)} + \mathbf{b}^{(k)}, \frac{1}{\rho_1 \|\mathbf{h}^{(k+1)}\|_2} \right)$$

$$\mathbf{b}^{(k+1)} = \mathbf{b}^{(k)} + \nabla u^{(k+1)} - \mathbf{d}^{(k+1)}$$

$$\mathbf{g}^{(k+1)} = \mathbf{g}^{(k)} + \nabla u^{(k+1)} - \mathbf{h}^{(k+1)}$$

$$w^{(k+1)} = w^{(k)} + f - Au^{(k+1)}$$

$$e^{(k+1)} = e^{(k)} + u^{(k+1)} - v^{(k+1)}$$

$$k = k + 1$$

end while

return $u^{(k)}$

4. Numerical experiments. In this section, we carry out a series of numerical tests to demonstrate the performance of the proposed L_1/L_2 models together with its corresponding algorithms. All the numerical experiments are conducted on a standard desktop with CPU (Intel i7-6700, 3.4GHz) and MATLAB 9.2 (R2017a).

We consider two types of sensing matrices: one is called oversampled discrete cosine transform (DCT) and the other is Gaussian matrix. Specifically for the oversampled DCT, we follow the works of [14, 26, 45] to define $A = [\mathbf{a}_1, \mathbf{a}_2, \dots, \mathbf{a}_n] \in \mathbb{R}^{m \times n}$ with

$$(4.1) \quad \mathbf{a}_j := \frac{1}{\sqrt{m}} \cos \left(\frac{2\pi \mathbf{w} j}{F} \right), \quad j = 1, \dots, n,$$

where \mathbf{w} is a random vector uniformly distributed in $[0, 1]^m$ and $F \in \mathbb{R}_+$ controls the coherence in a way that a larger value of F yields a more coherent matrix. In addition, we use $\mathcal{N}(\mathbf{0}, \Sigma)$ (the

multi-variable normal distribution) to generate Gaussian matrix, where the covariance matrix is $\Sigma = \{(1-r) * I(i=j) + r\}_{i,j}$ with a positive parameter r . This type of matrices is used in the TL1 paper [47], which mentioned that a larger r value indicates a more difficult problem in sparse recovery. Throughout the experiments, we consider sensing matrices of size 64×1024 . The ground truth $\mathbf{x} \in \mathbb{R}^n$ is simulated as s -sparse signal, where s is the total number of nonzero entries. The support of \mathbf{x} is a random index set and the values of non-zero elements follow Gaussian normal distribution i.e., $(\mathbf{x}_s)_i \sim \mathcal{N}(0, 1)$, $i = 1, 2, \dots, s$. We then normalize the ground-truth signal to have maximum magnitude as 1 so that we can examine the performance of additional $[-1, 1]$ box constraint.

Due to the non-convex nature of the proposed L_1/L_2 model, the initial guess $\mathbf{x}^{(0)}$ is very important and should be well-chosen. A typical choice is the L_1 solution (1.2), which is used here. We adopt a commercial optimization software called Gurobi [32] to minimize the L_1 norm via linear programming for the sake of efficiency. The stopping criterion is when the relative error of $\mathbf{x}^{(k)}$ to $\mathbf{x}^{(k-1)}$ is smaller than 10^{-8} or iterative number exceeds $10n$.

4.1. Algorithmic behaviors. We empirically demonstrate the convergence of the proposed ADMM algorithms in Figure 2. Specifically we examine the L_1/L_2 minimization problem (3.1), where the sensing matrix is an oversampled DCT matrix with $F = 10$ and ground-truth sparse vector has 12 non-zero elements. We also study the MRI reconstruction from 7 radial lines as a particular sparse gradient problem that involves the L_1/L_2 -grad minimization of (3.17) by Algorithm 3.2.

There are two auxiliary variables \mathbf{y} and \mathbf{z} in L_1/L_2 such that $\mathbf{x} = \mathbf{y} = \mathbf{z}$, while two auxiliary variables \mathbf{d}, \mathbf{h} are in L_1/L_2 -grad for $\nabla u = \mathbf{d} = \mathbf{h}$. We show in the top row of Figure 2 the values of $\|\mathbf{x}^{(k)} - \mathbf{y}^{(k)}\|_2$ and $\|\mathbf{x}^{(k)} - \mathbf{z}^{(k)}\|_2$ as well as $\|\nabla u^{(k)} - \mathbf{d}^{(k)}\|_2$ and $\|\nabla u^{(k)} - \mathbf{h}^{(k)}\|_2$, all are plotted with respect to the iteration counter k . The bottom row of Figure 2 is for objective functions, i.e., $\|\mathbf{x}^{(k)}\|_1 / \|\mathbf{x}^{(k)}\|_2$ and $\|\nabla u^{(k)}\|_1 / \|\nabla u^{(k)}\|_2$ for L_1/L_2 and L_1/L_2 -grad, respectively. All the plots in Figure 2 decrease rapidly with respect to iteration counters, which serves as heuristic evidence of algorithmic convergence. On the other hand, the objective functions in Figure 2 look oscillatory. This phenomenon implies difficulties in theoretically proving the convergence, as one key step in the convergence proof requires to show that objective function decreases monotonically [3, 42].

4.2. Comparison on various models. We now compare the proposed L_1/L_2 approach with other sparse recovery models: L_1 , L_p [9], L_1-L_2 [45, 26], and TL1 [47]. We choose $p = 0.5$ for L_p and $a = 1$ for TL1. The initial guess for all the algorithms is the solution of the L_1 model. Both L_1-L_2 and TL1 are solved via the DCA, with the same stopping criterion as L_1/L_2 , i.e., $\frac{\|\mathbf{x}^{(k)} - \mathbf{x}^{(k-1)}\|_2}{\|\mathbf{x}^{(k)}\|_2} \leq 10^{-8}$. As for L_p , we follow the default setting in [9].

We evaluate the performance of sparse recovery in terms of *success rate*, defined as the number of successful trials over the total number of trials. A success is declared if the relative error of the reconstructed solution \mathbf{x}^* to the ground truth \mathbf{x} is less than 10^{-3} , i.e., $\frac{\|\mathbf{x}^* - \mathbf{x}\|_2}{\|\mathbf{x}\|_2} \leq 10^{-3}$. We further categorize the failure of not recovering the ground-truth as *model failure* and *algorithm failure*. In particular, we compare the objective function $\mathcal{F}(\cdot)$ at the ground-truth \mathbf{x} and at the reconstructed solution \mathbf{x}^* . If $\mathcal{F}(\mathbf{x}) > \mathcal{F}(\mathbf{x}^*)$, it means that \mathbf{x} is not a global minimizer of the model, in which case we call *model failure*. On the other hand, $\mathcal{F}(\mathbf{x}) < \mathcal{F}(\mathbf{x}^*)$ implies that the algorithm does not reach a global minimizer, which is referred to as *algorithm failure*. Although this type of analysis is not deterministic, it sheds some lights on which direction to improve: model or algorithm. For example, it was reported in [30] that L_1 has the highest model-failure rates, which justifies the need

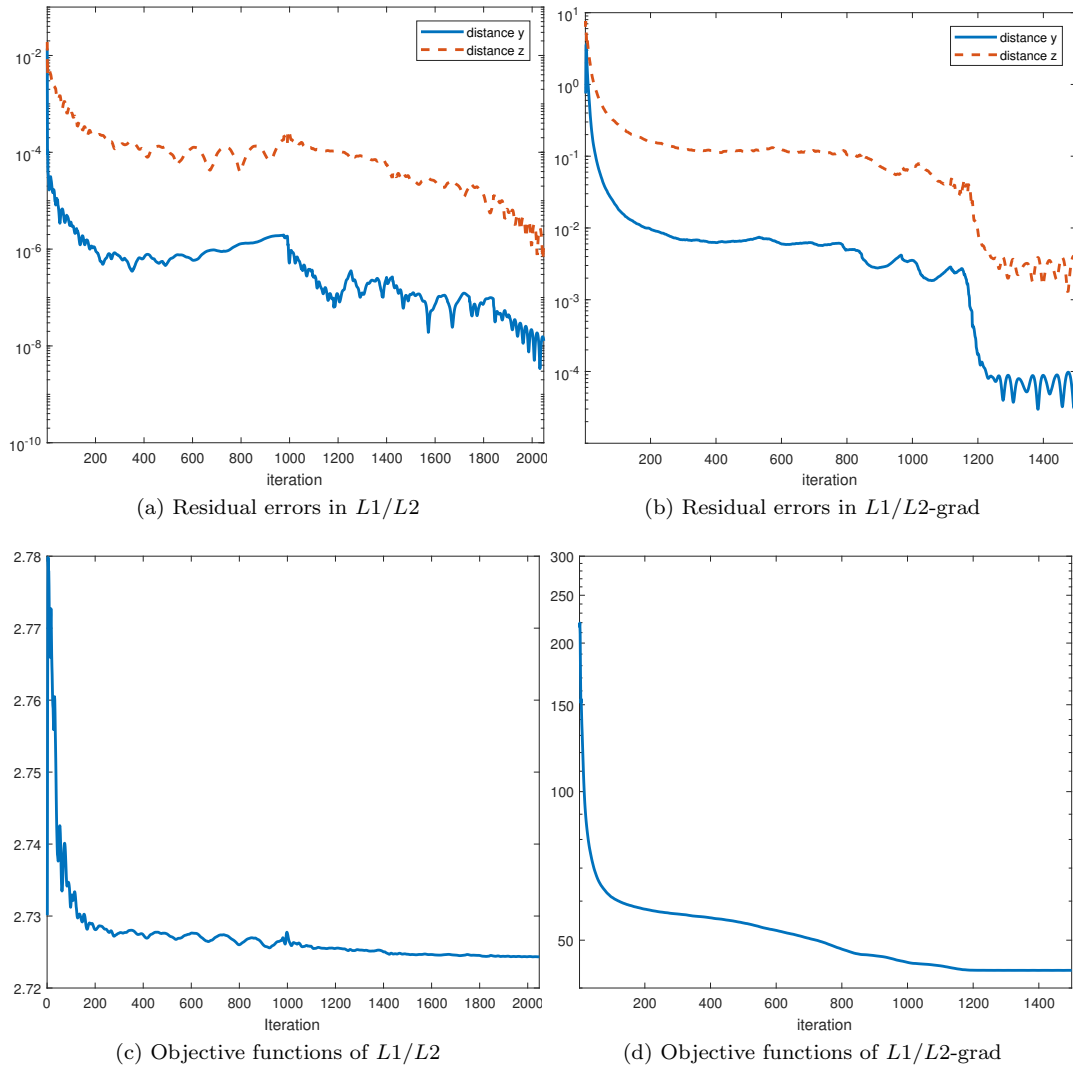


FIG. 2. Plots of residual errors and objective functions for empirically demonstrating the convergence of the proposed algorithms - L_1/L_2 in signal processing and L_1/L_2 -grad with a box constraint for MRI reconstruction.

for nonconvex models.

In Figure 3, we examine two coherence levels: $F = 5$ corresponds to relatively low coherence and $F = 20$ for higher coherence. The success rates of various models reveal that L_1/L_2 -box performs the best at $F = 5$ and is comparable to L_1-L_2 for the highly coherent case of $F = 20$. We look at Gaussian matrix with $r = 0.1$ and $r = 0.8$ in Figure 4, both of which exhibit very similar performance of various models. In particular, the L_p model gives the best results for the Gaussian case, which is consistent in the literature [44, 26]. The proposed model of L_1/L_2 -box is the second

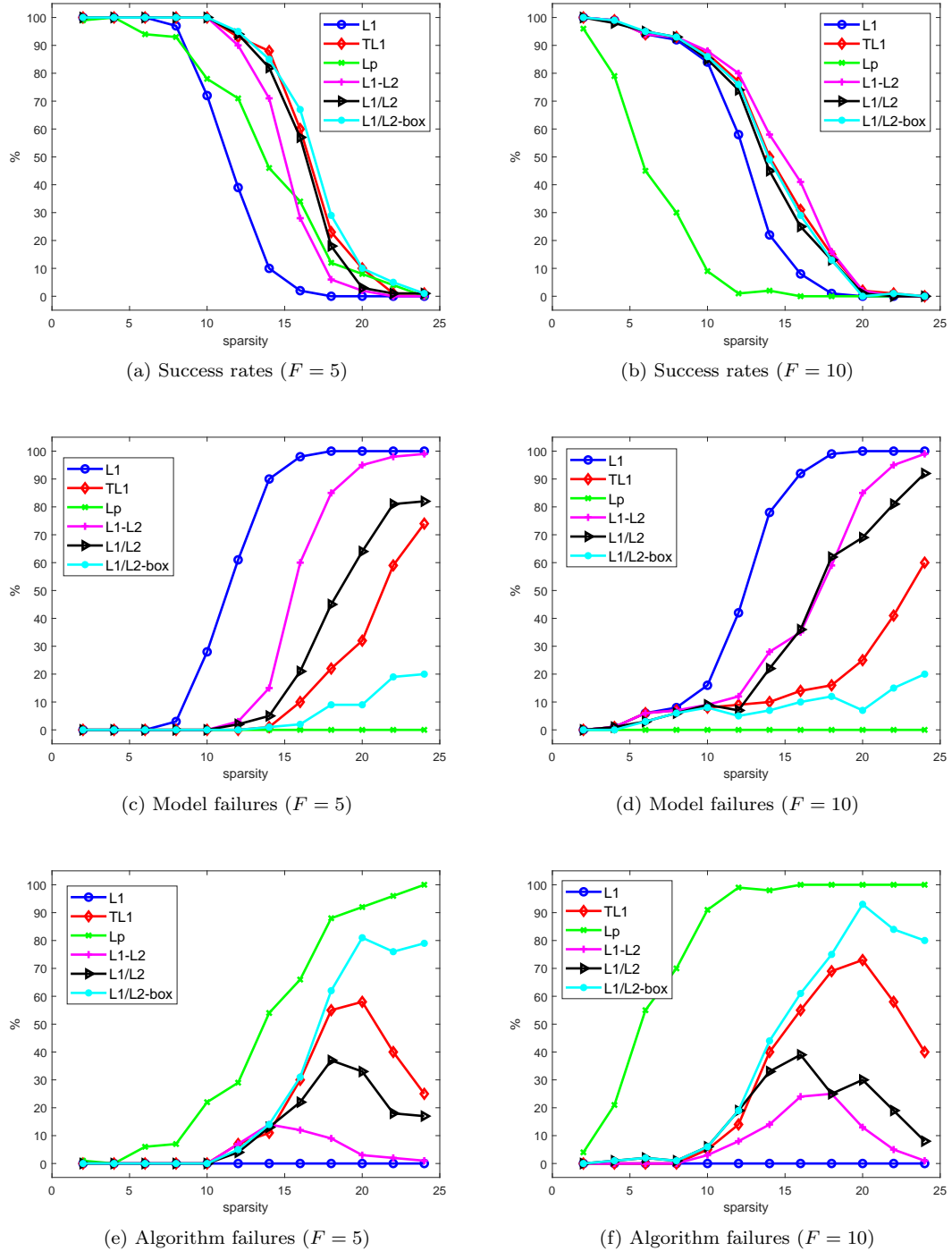


FIG. 3. Success rates, model failures, algorithm failures for 6 algorithms in the case of oversampled DCT matrices.

best for such incoherent matrices.

By comparing L_1/L_2 with and without box among the plots for success rates and model failures, we can draw the conclusion that the box constraint can mitigate the inherent drawback of the L_1/L_2 model, thus improving the recovery rates. In addition, L_1/L_2 is the second lowest in terms of model failure rates and simply adding a box constraint also increases the occurrence of algorithm failure compared to the none box version. These two observations suggest a need to further improve upon algorithms of minimizing L_1/L_2 .

Finally, we provide the computation time for all the competing algorithms in Table 1 with the shortest time in each case highlighted in bold. The time for L_1 method is not included, as all the other methods use the L_1 solution as initial guess. It is shown that TL1 is the fastest for relatively lower sparsity levels and the proposed L_1/L_2 -box is the most efficient at higher sparsity levels. The computational times for all these methods seem consistent with DCT and Gaussian matrices.

TABLE 1
Computation time (sec.) in 5 algorithms.

(a) DCT matrix

$F = 5$							
sparsity	2	6	10	14	18	22	mean
TL1	0.049	0.050	0.066	0.207	0.618	0.795	0.298
L_p	0.061	0.137	0.209	0.355	0.515	0.565	0.307
L_1-L_2	0.049	0.050	0.071	0.260	0.550	0.625	0.267
L_1/L_2	0.276	0.279	0.311	0.353	0.358	0.366	0.324
L_1/L_2 -box	0.102	0.183	0.247	0.313	0.325	0.332	0.250
$F = 10$							
sparsity	2	6	10	14	18	22	mean
TL1	0.048	0.069	0.092	0.330	0.654	0.755	0.325
L_p	0.094	0.254	0.423	0.472	0.530	0.534	0.385
L_1-L_2	0.049	0.070	0.093	0.272	0.598	0.677	0.293
L_1/L_2	0.263	0.272	0.295	0.340	0.355	0.356	0.314
L_1/L_2 -box	0.090	0.179	0.239	0.301	0.324	0.322	0.243

(b) Gaussian matrix

$r = 0.1$							
sparsity	2	6	10	14	18	22	mean
TL1	0.070	0.069	0.117	0.295	1.101	1.633	0.548
L_p	0.079	0.128	0.229	0.261	0.742	1.218	0.443
L_1-L_2	0.070	0.069	0.122	0.399	0.877	1.161	0.450
L_1/L_2	0.864	0.866	1.175	1.130	1.210	1.458	1.117
L_1/L_2 -box	0.324	0.625	1.039	1.060	1.146	1.385	0.930
$r = 0.8$							
sparsity	2	6	10	14	18	22	mean
TL1	0.050	0.053	0.071	0.239	0.613	0.750	0.296
L_p	0.061	0.094	0.140	0.207	0.426	0.613	0.257
L_1-L_2	0.051	0.054	0.077	0.306	0.497	0.576	0.260
L_1/L_2	0.277	0.277	0.324	0.358	0.364	0.363	0.327
L_1/L_2 -box	0.102	0.192	0.265	0.321	0.332	0.327	0.256

4.3. MRI reconstruction. As a proof-of-concept example, we study an MRI reconstruction problem [28] to compare the performance of L_1 , L_1-L_2 , and L_1/L_2 on the gradient. The L_1 on

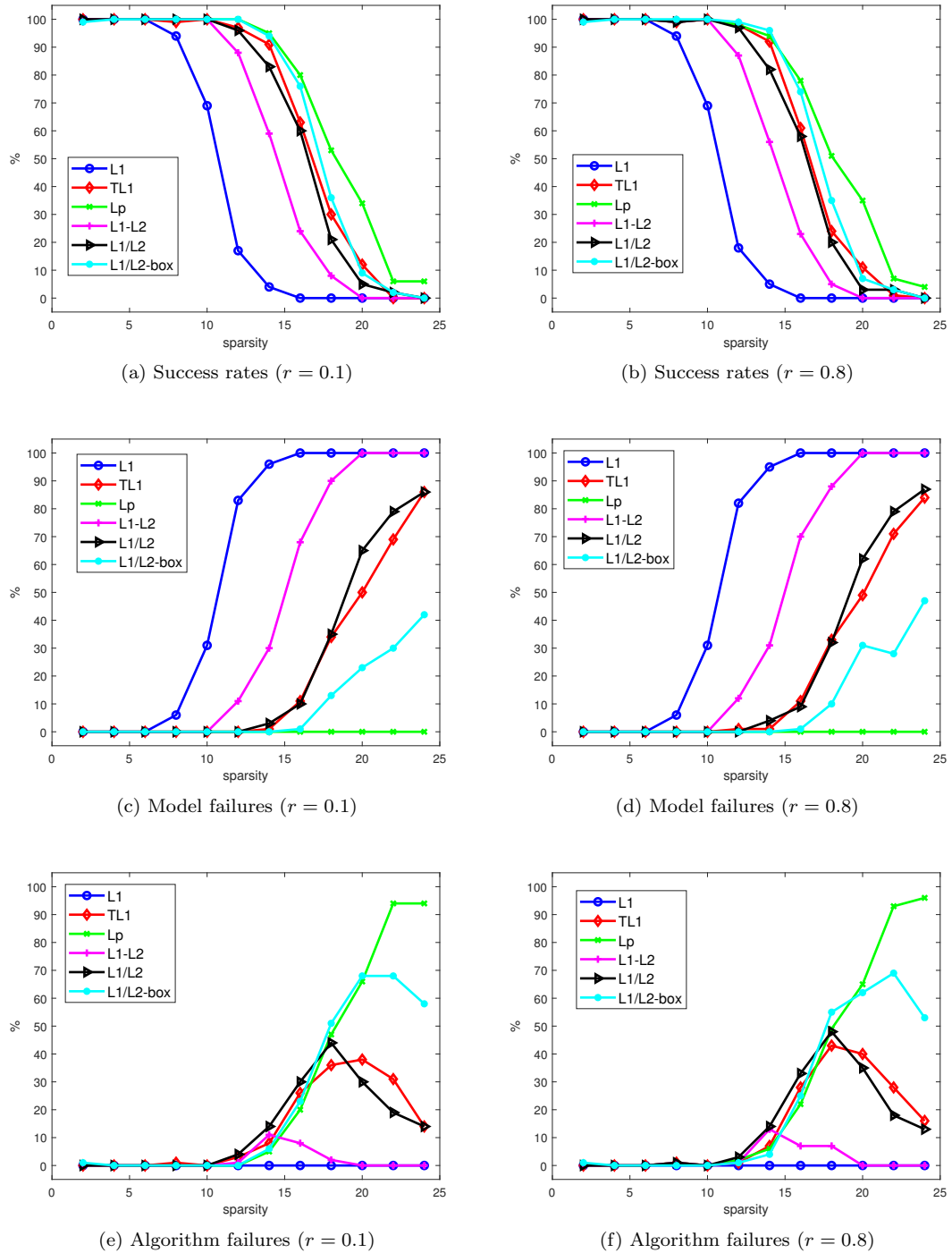


FIG. 4. Success rates, model failures, algorithm failures for 6 algorithms in the Gaussian matrix case.

the gradient is the celebrated TV model [36], while L_1 - L_2 on the gradient was recently proposed in [27]. We use a standard Shepp-Logan phantom as a testing image, as shown in Figure 5a. The MRI measurements are obtained by several radical lines in the frequency domain (i.e., after taking the Fourier transform); an example of such sampling scheme using 6 lines is shown in Figure 5b. As this paper focuses on the constrained formulation, we do not consider noise, following the same setting as in the previous works [45, 27]. Since all the competing methods (L_1 , L_1 - $0.5L_2$, and L_1/L_2) yield an exact recovery with 8 radical lines, with accuracy in the order of 10^{-8} , we present the reconstructions results of 6 radical lines in Figure 5, which illustrates that the ratio model (L_1/L_2) gives much better results than the difference model (L_1 - $0.5L_2$). Figure 5 also includes quantitative measures of the performance by relative error (RE) between the reconstructed and ground-truth images, which shows significantly improvement of the proposed L_1/L_2 -grad over a classic method in MRI reconstruction, called filter-back projection (FBP), and two recent works of using L_1 [15] and L_1 - $0.5L_2$ [27] on the gradient. Note that the state-of-the-art methods in MRI reconstruction are [18, 30] that have reported exact recovery from 7 radical lines.

5. Empirical validations. A review article [7] indicated that two principles in CS are *sparsity* and *incoherence*, leading an impression that a sensing matrix with smaller coherence is easier for sparse recovery. However, we observe through numerical results [25] (also given in Figure 6b) that a more coherent matrix gives higher recovery rates. This contradiction motivates us to collect empirical evidence regarding to either prove or refuse whether coherence is relevant to sparse recovery. Here we examine one such evidence by minimizing the ratio of L_1 and L_2 , which gives an upper bound for a sufficient condition of L_1 exact recovery, see (1.4). To avoid the trivial solution of $\mathbf{x} = \mathbf{0}$ to the problem of $\min_{\mathbf{x}} \left\{ \frac{\|\mathbf{x}\|_1}{\|\mathbf{x}\|_2} : \mathbf{A}\mathbf{x} = \mathbf{0} \right\}$, we incorporate a sum-to-one constraint. In other word, we define an expanded matrix $\tilde{\mathbf{A}} = [\mathbf{A}; \text{ones}(n, 1)]$ (following Matlab’s notation) and an expanded vector $\tilde{\mathbf{b}} = [\mathbf{0}; 1]$. We then adapt the proposed method to solve for $\min_{\mathbf{x}} \left\{ \frac{\|\mathbf{x}\|_1}{\|\mathbf{x}\|_2} : \tilde{\mathbf{A}}\mathbf{x} = \tilde{\mathbf{b}} \right\}$. In Figure 6a, we plot the mean value of ratios from 50 random realizations of matrices \mathbf{A} at each coherence level (controlled by F), which shows that the ratio actually decreases² with respect to F . As the L_0 norm is bounded by the ratio (1.4), smaller ratio indicates it is more difficult to recover the signals. Therefore, Figure 6a is consistent with the common belief in CS.

We postulate that an underlying reason of more coherent matrices giving better results is minimum separation (MS), as formally introduced in [5]. In Figure 6b, we enforce the minimum separation of two neighboring spikes to be 40, following the suggestion of $2F$ in [14] (we consider F up to 20). In comparison, we also give the success rates of the L_1 recovery without any restrictions on MS in Figure 6c. Note that we use the exactly same matrices in both cases (with and without MS). Figure 6c does not have a clear pattern regarding how coherence affects the exact recovery, which supports our hypothesis that minimum separation plays an important role in sparse recovery. It will be our future work to analyze it throughly.

6. Conclusions and future works. In this paper, we have studied a novel L_1/L_2 minimization to promote sparsity. Two main benefits of L_1/L_2 are scale invariant and parameter free. Two numerical algorithms based on the ADMM are formulated for the assumptions of sparse signals and sparse gradients, together with a variant of incorporating additional box constraint. The experimental results demonstrate the performance of the proposed approaches in comparison to the state-of-the-art methods in sparse recovery and MRI reconstruction. As a by-product, minimizing

²We also observe that the ratio stagnates for larger F , which is probably because of instability of the proposed method when matrix becomes more coherent.

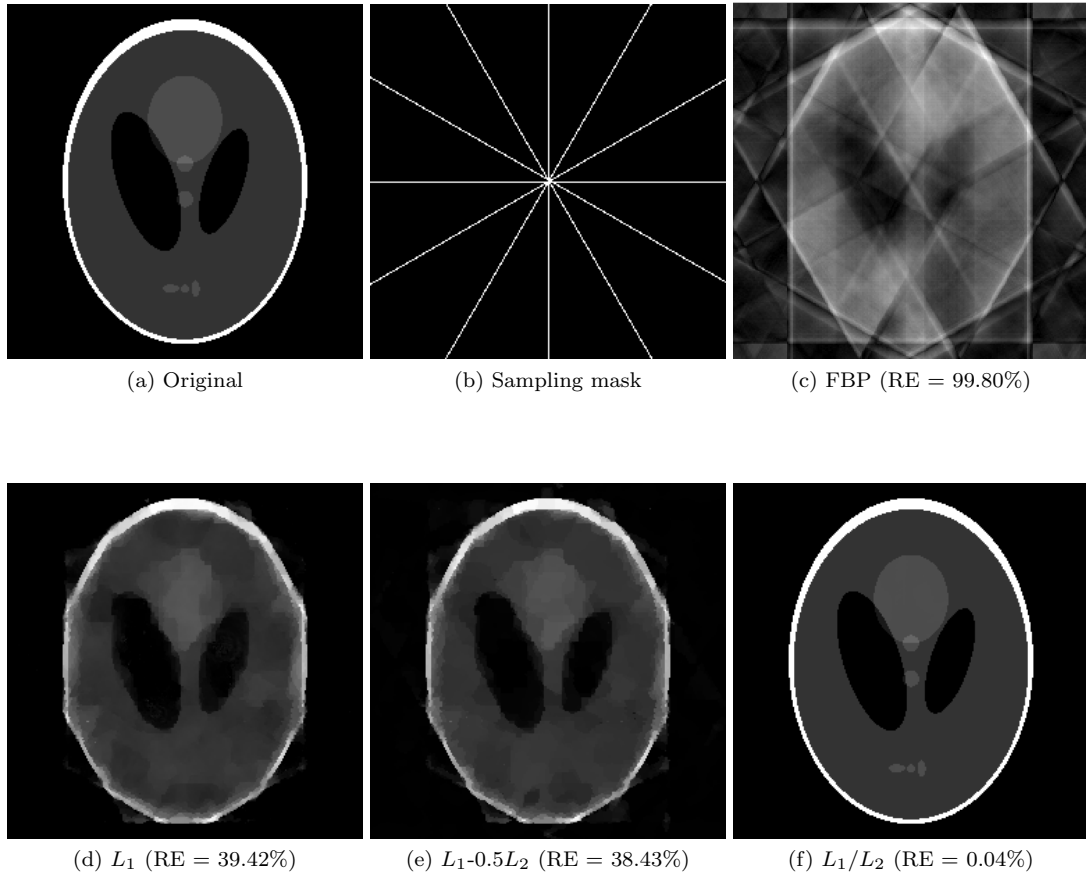


FIG. 5. MRI reconstruction results from 6 radical lines in the frequency domain (2.57% measurements). The relative errors (RE) are provided for each method.

the ratio also gives an empirical upper bound towards L_1 's exact recovery, which motivates further investigations on exact recovery theories. Other future works include algorithmic improvement and convergence analysis. In particular, it is shown in Table 1, Figures 3 and 4 that L_1/L_2 is not as fast as competing methods in CS and also has certain algorithmic failures, which calls for a more robust and more efficient algorithm. In addition, we have provided heuristic evidence of the ADMM's convergence in Figure 2 and it will be interesting to analyze it theoretically.

Acknowledgements. We would like to thank the editor and two reviewers for careful and thoughtful comments, which helped us greatly improve our paper. We also acknowledge the help of Dr. Min Tao from Nanjing University, who suggested the reference on the ADMM convergence.

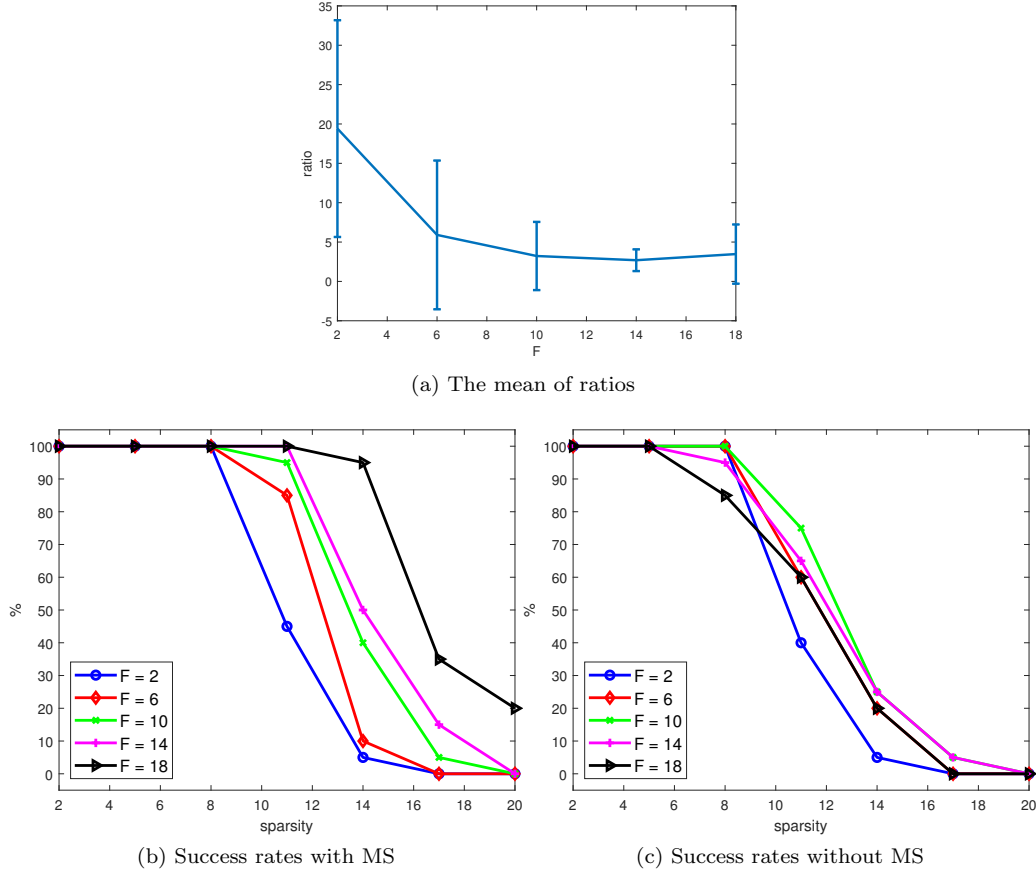


FIG. 6. The use of $\min_{\mathbf{x}} \left\{ \frac{\|\mathbf{x}\|_1}{\|\mathbf{x}\|_2} : \mathbf{A}\mathbf{x} = \mathbf{0} \right\}$ as an upper bound for the L_1 recovery. (a) plots the mean of ratios over 50 realizations with the standard deviation indicated as vertical bars. (b) and (c) are success rates of L_1 recovery with and without minimum separation.

Appendix: proof of Theorem 2.2. In order to prove Theorem 2.2, we study the function

$$(6.1) \quad g(t) = \frac{\|\mathbf{x} + t\mathbf{v}\|_1^2}{\|\mathbf{x} + t\mathbf{v}\|_2^2},$$

where $\mathbf{x} \neq \mathbf{0}$ ³ and

$$(6.2) \quad \mathbf{v} \in \ker(A) \setminus \{\mathbf{0}\} \text{ with } \|\mathbf{v}\|_2 = 1.$$

Notice that the denominator of the function g is non-zero for all $t \in \mathbb{R}$. Otherwise, we have $\mathbf{x} + t\mathbf{v} = \mathbf{0}$ and hence $A\mathbf{x} + A(t\mathbf{v}) = A(\mathbf{0})$. Since $A\mathbf{x} = \mathbf{b}$ and $A\mathbf{v} = \mathbf{0}$, we get $\mathbf{b} = \mathbf{0}$ which is a contradiction. Therefore, the function g is continuous everywhere. Next, we introduce the following lemma to discuss the L_1 term in the numerator of g .

³We assume that $\mathbf{b} \neq \mathbf{0}$ so $\mathbf{x} = \mathbf{0}$ is not a solution to $A\mathbf{x} = \mathbf{b}$.

LEMMA 6.1. For any $\mathbf{x} \in \mathbb{R}^n$ and $\mathbf{v} \in \mathbb{R}^n$ satisfying (6.2), denote S as the support of \mathbf{x} and $t_0 := \min_{i \in S} |x_i|$. We have

$$(6.3) \quad \|\mathbf{x} + t\mathbf{v}\|_1 = \|\mathbf{x}\|_1 + t\sigma_t(\mathbf{v}) > 0, \quad \forall |t| < t_0,$$

where

$$(6.4) \quad \sigma_t(\mathbf{v}) = \sum_{i \in S} v_i \text{sign}(x_i) + \text{sign}(t) \|\mathbf{v}_{\bar{S}}\|_1.$$

Proof. Since $\mathbf{x} + t\mathbf{v} \neq \mathbf{0}$ for all $t \in \mathbb{R}$, we have $\|\mathbf{x} + t\mathbf{v}\|_1 > 0$. It follows from (6.2) that $|v_i| \leq 1$, $\forall i$. Then we get $\text{sign}(x_i + tv_i) = \text{sign}(x_i)$, $\forall i \in S$, as $|tv_i| < |x_i|$ for $|t| < t_0$. Therefore, we have

$$\begin{aligned} \|\mathbf{x} + t\mathbf{v}\|_1 &= \sum_{i \in S} |x_i + tv_i| + \sum_{i \notin S} |t| |v_i| \\ &= \sum_{i \in S} (x_i + tv_i) \text{sign}(x_i) + |t| \|\mathbf{v}_{\bar{S}}\|_1 \\ &= \sum_{i \in S} x_i \text{sign}(x_i) + t \sum_{i \in S} v_i \text{sign}(x_i) + |t| \|\mathbf{v}_{\bar{S}}\|_1 \\ &= \|\mathbf{x}\|_1 + t \sum_{i \in S} v_i \text{sign}(x_i) + |t| \|\mathbf{v}_{\bar{S}}\|_1 \\ &= \|\mathbf{x}\|_1 + t \left(\sum_{i \in S} v_i \text{sign}(x_i) + \text{sign}(t) \|\mathbf{v}_{\bar{S}}\|_1 \right), \end{aligned}$$

which implies (6.3) and hence Lemma 6.1 holds. \square

Notice that $\sigma_t(\mathbf{v})$ only relies on the sign of t , i.e., it is constant for $t > 0$ and $t < 0$. Therefore, $g(t)$ is differentiable on $0 < t < t_0$ and $-t_0 < t < 0$ (Note that when $t \neq 0$, g is not differentiable at the points where $x_i + tv_i = 0$). Some simple calculations lead to the derivative of g for $0 < t < t_0$ and $-t_0 < t < 0$,

$$\begin{aligned} (6.5) \quad g'(t) &= \frac{d}{dt} \left(\frac{(\|\mathbf{x}\|_1 + t\sigma_t(\mathbf{v}))^2}{\|\mathbf{x}\|_2^2 + 2t \langle \mathbf{v}_S, \mathbf{x} \rangle + t^2 \|\mathbf{v}\|_2^2} \right) \\ &= \frac{2\sigma_t(\mathbf{v}) (\|\mathbf{x}\|_1 + t\sigma_t(\mathbf{v})) (\|\mathbf{x}\|_2^2 + 2t \langle \mathbf{v}_S, \mathbf{x} \rangle + t^2 \|\mathbf{v}\|_2^2) - (2 \langle \mathbf{v}_S, \mathbf{x} \rangle + 2t \|\mathbf{v}\|_2^2) (\|\mathbf{x}\|_1 + t\sigma_t(\mathbf{v}))^2}{(\|\mathbf{x}\|_2^2 + 2t \langle \mathbf{v}_S, \mathbf{x} \rangle + t^2 \|\mathbf{v}\|_2^2)^2} \\ &= \frac{2 (\|\mathbf{x}\|_1 + t\sigma_t(\mathbf{v})) [\sigma_t(\mathbf{v}) (\|\mathbf{x}\|_2^2 + 2t \langle \mathbf{v}_S, \mathbf{x} \rangle + t^2 \|\mathbf{v}\|_2^2) - (\langle \mathbf{v}_S, \mathbf{x} \rangle + t \|\mathbf{v}\|_2^2) (\|\mathbf{x}\|_1 + t\sigma_t(\mathbf{v}))]}{(\|\mathbf{x}\|_2^2 + 2t \langle \mathbf{v}_S, \mathbf{x} \rangle + t^2 \|\mathbf{v}\|_2^2)^2} \\ &= \frac{2 (\|\mathbf{x}\|_1 + t\sigma_t(\mathbf{v})) [(\sigma_t(\mathbf{v}) \|\mathbf{x}\|_2^2 - \langle \mathbf{v}_S, \mathbf{x} \rangle \|\mathbf{x}\|_1) + (\sigma_t(\mathbf{v}) \langle \mathbf{v}_S, \mathbf{x} \rangle - \|\mathbf{x}\|_1 \|\mathbf{v}\|_2^2) t]}{(\|\mathbf{x}\|_2^2 + 2t \langle \mathbf{v}_S, \mathbf{x} \rangle + t^2 \|\mathbf{v}\|_2^2)^2}. \end{aligned}$$

It follows from Lemma 6.1 that the first term in the numerator of (6.5) is strictly positive, i.e., $\|\mathbf{x}\|_1 + t\sigma_t(\mathbf{v}) > 0$. Therefore, the sign of g' depends on the second term in the numerator. We further introduce two lemmas (Lemma 6.2 and Lemma 6.3) to study this term.

LEMMA 6.2. For any $\mathbf{x}, \mathbf{v} \in \mathbb{R}^n$ and $i \in [n]$, we have

$$(6.6) \quad n\|\mathbf{x}\|_2^2 - |x_i|\|\mathbf{x}\|_1 \geq (n-1) \left(\sum_{j \neq i} x_j^2 \right),$$

$$(6.7) \quad n\|\mathbf{v}\|_1\|\mathbf{x}\|_2^2 \geq \|\mathbf{x}\|_1 |\langle \mathbf{v}, \mathbf{x} \rangle|.$$

Furthermore, if $\|\mathbf{x}\|_0 = s$, then the constant n in the inequalities can be reduced to s .

Proof. Simple calculations show that

$$(6.8) \quad \begin{aligned} n\|\mathbf{x}\|_2^2 - |x_i|\|\mathbf{x}\|_1 &= n \left(\sum_j x_j^2 \right) - |x_i| \left(\sum_j |x_j| \right) \\ &= (n-1) \left(\sum_{j \neq i} x_j^2 \right) + \sum_{j \neq i} x_j^2 + (n-1)x_i^2 - \sum_{j \neq i} |x_i||x_j| \\ &= (n-1) \left(\sum_{j \neq i} x_j^2 \right) + \sum_{j \neq i} (|x_i| - |x_j|)^2 + |x_i||x_j| \\ &\geq (n-1) \left(\sum_{j \neq i} x_j^2 \right) \geq 0. \end{aligned}$$

Therefore, we have $\sum_i (n\|\mathbf{x}\|_2^2 - |x_i|\|\mathbf{x}\|_1) |v_i| \geq 0$, which implies that

$$(6.9) \quad n\|\mathbf{v}\|_1\|\mathbf{x}\|_2^2 \geq \|\mathbf{x}\|_1 \left(\sum_i |x_i||v_i| \right) \geq \|\mathbf{x}\|_1 |\langle \mathbf{v}, \mathbf{x} \rangle|.$$

Similarly, we can reduce the constant n to s , if we know $\|\mathbf{x}\|_0 = s$. \square

LEMMA 6.3. Suppose that an s -sparse vector \mathbf{x} satisfies $A\mathbf{x} = \mathbf{b}$ ($\mathbf{b} \neq 0$) with its support on an index set S and the matrix A satisfies the s NSP of order s . Define

$$(6.10) \quad t_1 := \inf_{\mathbf{v}, t} \left\{ \frac{|\sigma_t(\mathbf{v})\|\mathbf{x}\|_2^2 - \langle \mathbf{v}_S, \mathbf{x} \rangle \|\mathbf{x}\|_1|}{|\sigma_t(\mathbf{v}) \langle \mathbf{v}_S, \mathbf{x} \rangle - \|\mathbf{x}\|_1\|\mathbf{v}\|_2^2|} \mid \mathbf{v} \in \ker(A), \|\mathbf{v}\|_2 = 1, t \neq 0 \right\},$$

where $\sigma_t(\mathbf{v})$ is defined as (6.4). Then $t_1 > 0$.

Proof. For any $\mathbf{v} \in \ker(A)$ and $\|\mathbf{v}\|_2 = 1$, it is straightforward that

$$(6.11) \quad \begin{aligned} |\sigma_t(\mathbf{v}) \langle \mathbf{v}_S, \mathbf{x} \rangle - \|\mathbf{x}\|_1\|\mathbf{v}\|_2^2| &\leq |\sigma_t(\mathbf{v})|\|\mathbf{v}\|_2\|\mathbf{x}\|_2 + \|\mathbf{x}\|_1\|\mathbf{v}\|_2^2 \\ &\leq \|\mathbf{v}\|_1\|\mathbf{v}\|_2\|\mathbf{x}\|_2 + \|\mathbf{x}\|_1\|\mathbf{v}\|_2^2 \\ &= \|\mathbf{v}\|_1\|\mathbf{x}\|_2 + \|\mathbf{x}\|_1 \\ &\leq \sqrt{n}\|\mathbf{x}\|_2 + \|\mathbf{x}\|_1, \end{aligned}$$

and

$$(6.12) \quad |\sigma_t(\mathbf{v})| \geq |\text{sign}(t)|\|\mathbf{v}_{\bar{S}}\|_1 - \left| \sum_{i \in S} v_i \text{sign}(x_i) \right| \geq \|\mathbf{v}_{\bar{S}}\|_1 - \sum_{i \in S} |v_i| = \|\mathbf{v}_{\bar{S}}\|_1 - \|\mathbf{v}_S\|_1.$$

It follows from the sNSP that $\|\mathbf{v}_{\bar{S}}\|_1 \geq (s+1)\|\mathbf{v}_S\|_1$, thus leading to the following two inequalities,

$$(6.13) \quad \begin{aligned} |\sigma_t(\mathbf{v})| &\geq \|\mathbf{v}_{\bar{S}}\|_1 - \|\mathbf{v}_S\|_1 \geq s\|\mathbf{v}_S\|_1 \\ |\sigma_t(\mathbf{v})| &\geq \|\mathbf{v}_{\bar{S}}\|_1 - \|\mathbf{v}_S\|_1 \geq \left(1 - \frac{1}{s+1}\right)\|\mathbf{v}_{\bar{S}}\|_1 = \frac{s}{s+1}\|\mathbf{v}_{\bar{S}}\|_1. \end{aligned}$$

Next we will discuss two cases: $s = 1$ and $s > 1$.

- (i) For $s = 1$. Without loss of generality, we assume the only non-zero element is $x_n \neq 0$ and hence we have

$$|\sigma_t(\mathbf{v})\|\mathbf{x}\|_2^2 - \langle \mathbf{v}_S, \mathbf{x} \rangle \|\mathbf{x}\|_1 = |(v_n \text{sign}(x_n) + \text{sign}(t)\|\mathbf{v}_{\bar{S}}\|_1)x_n^2 - (v_n x_n)|x_n| = \|\mathbf{v}_{\bar{S}}\|_1 x_n^2.$$

We further discuss two cases: $|v_n| \geq \frac{1}{\sqrt{n}}$ and $|v_n| < \frac{1}{\sqrt{n}}$. If $|v_n| \geq \frac{1}{\sqrt{n}}$, then $\|\mathbf{v}_{\bar{S}}\|_1 \geq (s+1)|v_n| \geq \frac{s+1}{\sqrt{n}}$ and hence

$$(6.14) \quad |\sigma_t(\mathbf{v})\|\mathbf{x}\|_2^2 - \langle \mathbf{v}_S, \mathbf{x} \rangle \|\mathbf{x}\|_1 = \|\mathbf{v}_{\bar{S}}\|_1 \|\mathbf{x}\|_2^2 \geq \frac{s+1}{\sqrt{n}} \|\mathbf{x}\|_2^2.$$

If $|v_n| < \frac{1}{\sqrt{n}}$, then we have $\|\mathbf{v}_{\bar{S}}\|_1 \geq 1 - |v_n| = 1 - \frac{1}{\sqrt{n}} = \frac{\sqrt{n}-1}{\sqrt{n}}$ and

$$(6.15) \quad |\sigma_t(\mathbf{v})\|\mathbf{x}\|_2^2 - \langle \mathbf{v}_S, \mathbf{x} \rangle \|\mathbf{x}\|_1 = \|\mathbf{v}_{\bar{S}}\|_1 \|\mathbf{x}\|_2^2 \geq \frac{\sqrt{n}-1}{\sqrt{n}} \|\mathbf{x}\|_2^2.$$

Combining (6.14) and (6.15), we have

$$(6.16) \quad t_1 \geq \frac{\min\left\{\frac{s+1}{\sqrt{n}}\|\mathbf{x}\|_2^2, \frac{\sqrt{n}-1}{\sqrt{n}}\|\mathbf{x}\|_2^2\right\}}{\sqrt{n}\|\mathbf{x}\|_2 + \|\mathbf{x}\|_1} > 0.$$

- (ii) For $s > 1$. We split into two cases. The first case is $\forall j \in S, v_j < c$ (we will determine the value of c shortly). As a result, we get $\|\mathbf{v}_S\|_1 < sc$ and $\|\mathbf{v}_{\bar{S}}\|_1 \geq 1 - sc$ since $\|\mathbf{v}\|_1 \geq \|\mathbf{v}\|_2 = 1$. Some simple calculations lead to

$$\begin{aligned} |\sigma_t(\mathbf{v})\|\mathbf{x}\|_2^2 - \langle \mathbf{v}_S, \mathbf{x} \rangle \|\mathbf{x}\|_1 &\geq |\sigma_t(\mathbf{v})\|\mathbf{x}\|_2^2 - |\langle \mathbf{v}_S, \mathbf{x} \rangle \|\mathbf{x}\|_1 \\ &\geq \frac{s}{s+1}\|\mathbf{v}_{\bar{S}}\|_1 \|\mathbf{x}\|_2^2 - \sum_{i \in S} |v_i| |x_i| |x|_1 \quad (\text{based on (6.13)}) \\ &\geq \frac{s}{s+1}(1 - sc)\|\mathbf{x}\|_2^2 - \sum_{i \in S} c |x_i| \|\mathbf{x}\|_1 \\ &= \frac{s}{s+1}(1 - sc)\|\mathbf{x}\|_2^2 - c\|\mathbf{x}\|_1^2 \\ &\geq \frac{s}{s+1}(1 - su_0)\|\mathbf{x}\|_2^2 - sc\|\mathbf{x}\|_2^2 \\ &= \frac{s}{s+1}(1 - (2s+1)c)\|\mathbf{x}\|_2^2. \end{aligned}$$

If we choose $c = \frac{1}{2s+2}$, then the above quantity is larger than $\frac{s\|\mathbf{x}\|_2^2}{(s+1)(2s+2)} > 0$.

In the second case, we have there exist $j \in S$ such that $v_j \geq c$, leading to

$$\begin{aligned}
(6.17) \quad & |\sigma_t(\mathbf{v})\|\mathbf{x}\|_2^2 - \langle \mathbf{v}_S, \mathbf{x} \rangle \|\mathbf{x}\|_1| \geq |\sigma_t(\mathbf{v})\|\mathbf{x}\|_2^2 - \langle \mathbf{v}_S, \mathbf{x} \rangle \|\mathbf{x}\|_1 \\
& \geq s\|\mathbf{v}_S\|_1\|\mathbf{x}\|_2^2 - \left(\sum_{i \in S} |x_i| |v_i| \right) \|\mathbf{x}\|_1 \\
& = \sum_{i \in S} (s\|\mathbf{x}\|_2^2 - |x_i| \|\mathbf{x}\|_1) |v_i| \\
& \geq (s\|\mathbf{x}\|_2^2 - |x_j| \|\mathbf{x}\|_1) |v_j| \quad (\text{based on Lemma 6.2}) \\
& \geq c (s\|\mathbf{x}\|_2^2 - |x_j| \|\mathbf{x}\|_1) \\
& \geq c(s-1) \sum_{i \neq j} x_i^2 \quad (\text{based on Lemma 6.2}) \\
& \geq c(s-1) \min_{j \in S} \sum_{i \neq j} x_i^2.
\end{aligned}$$

These two cases guarantee that $t_1 > 0$, i.e.,

$$(6.18) \quad t_1 \geq \frac{\min \left\{ c(s-1) \min_{j \in S} \sum_{i \neq j} x_i^2, \frac{s\|\mathbf{x}\|_2^2}{(s+1)(2s+2)} \right\}}{\sqrt{n}\|\mathbf{x}\|_2 + \|\mathbf{x}\|_1} > 0.$$

By (6.16) and (6.18), we get Lemma 6.3. \square

Now, we are ready to prove Theorem 2.2.

Proof. According to (6.3), the first term in the numerator is strictly positive, i.e., $\|\mathbf{x}\|_1 + t\sigma_t(\mathbf{v}) = \|\mathbf{x} + t\mathbf{v}\|_1 > 0$, $\forall |t| < t_0$. As for the second one, there exists a positive number t_1 defined in Lemma 6.3 such that

$$|\sigma_t(\mathbf{v}) \langle \mathbf{v}_S, \mathbf{x} \rangle - \|\mathbf{x}\|_1 \|\mathbf{v}\|_2^2| |t| < |\sigma_t(\mathbf{v})\|\mathbf{x}\|_2^2 - \langle \mathbf{v}_S, \mathbf{x} \rangle \|\mathbf{x}\|_1|$$

for all $|t| < t_1$ and $\mathbf{v} \in \ker(A)$ with $\|\mathbf{v}\|_2 = 1$. Moreover, we have

$$\begin{aligned}
& \text{sign} \left[(\sigma_t(\mathbf{v})\|\mathbf{x}\|_2^2 - \langle \mathbf{v}_S, \mathbf{x} \rangle \|\mathbf{x}\|_1 + (\sigma_t(\mathbf{v}) \langle \mathbf{v}_S, \mathbf{x} \rangle - \|\mathbf{x}\|_1 \|\mathbf{v}\|_2^2) t) \right] \\
& = \text{sign} \left(\sigma_t(\mathbf{v})\|\mathbf{x}\|_2^2 - \langle \mathbf{v}_S, \mathbf{x} \rangle \|\mathbf{x}\|_1 \right).
\end{aligned}$$

Letting $t^* = \min\{t_0, t_1\}$, we have for any $t \in (0, t^*)$ and $\mathbf{v} \neq \mathbf{0}$ that $\sigma_t(\mathbf{v}) > 0$ as

$$\begin{aligned}
(6.19) \quad & \sigma_t(\mathbf{v}) = \sum_{i \in S} v_i \text{sign}(x_i) + \text{sign}(t) \|\mathbf{v}_S\|_1 \\
& = \sum_{i \in S} v_i \text{sign}(x_i) + \|\mathbf{v}_S\|_1 \\
& \geq \|\mathbf{v}_S\|_1 - \|\mathbf{v}_S\|_1 \\
& \geq \max \left\{ s\|\mathbf{v}_S\|_1, \frac{s}{s+1} \|\mathbf{v}_S\|_1 \right\} > 0 \quad (\text{based on (6.13)}).
\end{aligned}$$

Also (6.13) implies that

$$(6.20) \quad |\sigma_t(\mathbf{v})| \|\mathbf{x}\|_2^2 \geq s \|\mathbf{v}_S\|_1 \|\mathbf{x}\|_2^2 \geq \|\mathbf{v}_S\|_1 \|\mathbf{x}\|_1^2 \geq |\langle \mathbf{v}_S, \mathbf{x} \rangle| \|\mathbf{x}\|_1,$$

thus leading to

$$(6.21) \quad \sigma_t(\mathbf{v}) \|\mathbf{x}\|_2^2 - \langle \mathbf{v}_S, \mathbf{x} \rangle \|\mathbf{x}\|_1 \geq 0,$$

for $\sigma_t(\mathbf{v}) > 0$. As a result, we have $g'(t) \geq 0$ if $0 < t < t^*$. The function $g(t)$ is not differentiable at zero, but we can compute the sub-derivative as follows,

$$(6.22) \quad g'(0^+) = \lim_{t \rightarrow 0^+} \frac{g(t) - g(0)}{t - 0} = \frac{2\|\mathbf{x}\|_1 (\sigma_{+1}(\mathbf{v}) \|\mathbf{x}\|_2^2 - \langle \mathbf{v}_S, \mathbf{x} \rangle \|\mathbf{x}\|_1)}{\|\mathbf{x}\|_2^4} \geq 0.$$

Similarly, we can get $g'(t) \leq 0$ if $-t^* < t < 0$ and $g'(0^-) \leq 0$. Therefore for any $0 < |t| < t^*$ we have $g(0) \leq g(t)$, which implies that

$$(6.23) \quad \frac{\|\mathbf{x} + t\mathbf{v}\|_1}{\|\mathbf{x} + t\mathbf{v}\|_2} \geq \frac{\|\mathbf{x}\|_1}{\|\mathbf{x}\|_2}, \quad \forall |t| < t^*. \quad \square$$

Notice that t^* does not depend on the choice of \mathbf{v} , therefore the inequality is true for any \mathbf{v} satisfying 6.2, which will imply the result.

REFERENCES

- [1] A. S. BANDEIRA, E. DOBRIBAN, D. G. MIXON, AND W. F. SAWIN, *Certifying the restricted isometry property is hard*, IEEE Trans. Inf. Theory, 59 (2013), pp. 3448–3450.
- [2] A. BECK, *First-Order Methods in Optimization*, vol. 25, SIAM, 2017.
- [3] J. BOLTE, S. SABACH, AND M. TEBoulLE, *Proximal alternating linearized minimization for nonconvex and nonsmooth problems*, Math. Program., 146 (2014), pp. 459–494.
- [4] S. BOYD, N. PARIKH, E. CHU, B. PELEATO, AND J. ECKSTEIN, *Distributed optimization and statistical learning via the alternating direction method of multipliers*, Found. Trends Mach. Learn., 3 (2011), pp. 1–122.
- [5] E. J. CANDÈS AND C. FERNANDEZ-GRANDA, *Towards a mathematical theory of super-resolution*, Comm. Pure Appl. Math., 67 (2014), pp. 906–956.
- [6] E. J. CANDÈS, J. ROMBERG, AND T. TAO, *Stable signal recovery from incomplete and inaccurate measurements*, Comm. Pure Appl. Math., 59 (2006), pp. 1207–1223.
- [7] E. J. CANDÈS AND M. B. WAKIN, *An introduction to compressive sampling*, IEEE Signal Process. Mag., 25 (2008), pp. 21–30.
- [8] A. CHAMBOLLE AND T. POCK, *A first-order primal-dual algorithm for convex problems with applications to imaging*, J. Math. Imaging and Vision, 40 (2011), pp. 120–145.
- [9] R. CHARTRAND, *Exact reconstruction of sparse signals via nonconvex minimization*, IEEE Signal Process. Lett., 10 (2007), pp. 707–710.
- [10] A. COHEN, W. DAHMEN, AND R. DEVORE, *Compressed sensing and the best k -term approximation*, J. Am. Math. Soc., 22 (2009), pp. 211–231.
- [11] D. DONOHO AND M. ELAD, *Optimally sparse representation in general (nonorthogonal) dictionaries via l_1 minimization*, Proc. Nat. Acad. Scien. USA, 100 (2003), pp. 2197–2202.
- [12] D. L. DONOHO AND X. HUO, *Uncertainty principles and ideal atomic decomposition*, IEEE Trans. Inf. Theory, 47 (2001), pp. 2845–2862.
- [13] E. ESSER, Y. LOU, AND J. XIN, *A method for finding structured sparse solutions to non-negative least squares problems with applications*, SIAM J. Imaging Sci., 6 (2013), pp. 2010–2046.
- [14] A. FANNJIANG AND W. LIAO, *Coherence pattern-guided compressive sensing with unresolved grids*, SIAM J. Imaging Sci., 5 (2012), pp. 179–202.
- [15] T. GOLDSTEIN AND S. OSHER, *The split Bregman method for L_1 -regularized problems*, SIAM J. Imaging Sci., 2 (2009), pp. 323–343.

- [16] R. GRIBONVAL AND M. NIELSEN, *Sparse representations in unions of bases*, IEEE Trans. Inf. Theory, 49 (2003), pp. 3320–3325.
- [17] K. GUO, D. HAN, AND T.-T. WU, *Convergence of alternating direction method for minimizing sum of two nonconvex functions with linear constraints*, Int. J. of Comput. Math., 94 (2017), pp. 1653–1669.
- [18] W. GUO AND W. YIN, *Edge guided reconstruction for compressive imaging*, SIAM J. Sci. Imaging, 5 (2012), pp. 809–834.
- [19] M. HONG, Z.-Q. LUO, AND M. RAZAVIYAYN, *Convergence analysis of alternating direction method of multipliers for a family of nonconvex problems*, SIAM J. Optim., 26 (2016), pp. 337–364.
- [20] P. O. HOYER, *Non-negative sparse coding*, in Proc. IEEE Workshop Neural Networks Signal Proce., 2002, pp. 557–565.
- [21] N. HURLEY AND S. RICKARD, *Comparing measures of sparsity*, IEEE Trans. on Inform. Theory, 55 (2009), pp. 4723–4741.
- [22] D. KRISHNAN, T. TAY, AND R. FERGUS, *Blind deconvolution using a normalized sparsity measure*, in IEEE Conference on Computer Vision and Pattern Recognition (CVPR), IEEE, 2011, pp. 233–240.
- [23] M. J. LAI, Y. XU, AND W. YIN, *Improved iteratively reweighted least squares for unconstrained smoothed l_q minimization*, SIAM J. Numer. Anal., 5 (2013), pp. 927–957.
- [24] G. LI AND T. K. PONG, *Global convergence of splitting methods for nonconvex composite optimization*, SIAM J. Optim., 25 (2015), pp. 2434–2460.
- [25] Y. LOU, S. OSHER, AND J. XIN, *Computational aspects of L_1 - L_2 minimization for compressive sensing*, in Model. Comput. & Optim. in Inf. Syst. & Manage. Sci., Adv. Intel. Syst. Comput., vol. 359, 2015, pp. 169–180.
- [26] Y. LOU, P. YIN, Q. HE, AND J. XIN, *Computing sparse representation in a highly coherent dictionary based on difference of L_1 and L_2* , J. Sci. Comput., 64 (2015), pp. 178–196.
- [27] Y. LOU, T. ZENG, S. OSHER, AND J. XIN, *A weighted difference of anisotropic and isotropic total variation model for image processing*, SIAM J. Imaging Sci., 8 (2015), pp. 1798–1823.
- [28] M. LUSTIG, D. L. DONOHO, AND J. M. PAULY, *Sparse MRI: The application of compressed sensing for rapid MR imaging*, Magnet. Reson. Med., 58 (2007), pp. 1182–1195.
- [29] J. LV AND Y. FAN, *A unified approach to model selection and sparse recovery using regularized least squares*, Ann. Appl. Stat., (2009), pp. 3498–3528.
- [30] T. MA, Y. LOU, AND T. HUANG, *Truncated L_1 - L_2 models for sparse recovery and rank minimization*, SIAM J. Imaging Sci., 10 (2017), pp. 1346–1380.
- [31] B. K. NATARAJAN, *Sparse approximate solutions to linear systems*, SIAM J. Comput., (1995), pp. 227–234.
- [32] G. OPTIMIZATION, *Gurobi optimizer reference manual*, 2015.
- [33] J.-S. PANG AND M. TAO, *Decomposition methods for computing directional stationary solutions of a class of nonsmooth nonconvex optimization problems*, SIAM J. Optim., 28 (2018), pp. 1640–1669.
- [34] H. RAGUET, J. FADILI, AND G. PEYRE, *A generalized forward-backward splitting*, SIAM J. Imaging Sci., 6 (2013), pp. 1199–1226.
- [35] A. REPETTI, M. Q. PHAM, L. DUVAL, E. CHOUZENOUXE, AND J.-C. PESQUET, *Euclid in a taxicab: Sparse blind deconvolution with smoothed l_1/l_2 regularization*, IEEE Signal Process. Lett., 22 (2015), pp. 539–543.
- [36] L. RUDIN, S. OSHER, AND E. FATEMI, *Nonlinear total variation based noise removal algorithms*, Physica D, 60 (1992), pp. 259–268.
- [37] X. SHEN, W. PAN, AND Y. ZHU, *Likelihood-based selection and sharp parameter estimation*, J. Am. Stat. Assoc., 107 (2012), pp. 223–232.
- [38] A. M. TILLMANN AND M. E. PFETSCH, *The computational complexity of the restricted isometry property, the nullspace property, and related concepts in compressed sensing*, IEEE Trans. Inf. Theory, 60 (2014), pp. 1248–1259.
- [39] H. TRAN AND C. WEBSTER, *Unified sufficient conditions for uniform recovery of sparse signals via nonconvex minimizations*, arXiv preprint arXiv:1710.07348, (2017).
- [40] F. WANG, W. CAO, AND Z. XU, *Convergence of multi-block Bregman ADMM for nonconvex composite problems*, Sci. China Info. Sci., 61 (2018), pp. 122101:1–12.
- [41] F. WANG, Z. XU, AND H.-K. XU, *Convergence of Bregman alternating direction method with multipliers for nonconvex composite problems*, arXiv preprint arXiv:1410.8625, (2014).
- [42] Y. WANG, W. YIN, AND J. ZENG, *Global convergence of ADMM in nonconvex nonsmooth optimization*, J. Sci. Comput., 78 (2019), pp. 29–63.
- [43] Z. XU, X. CHANG, F. XU, AND H. ZHANG, *$l_{1/2}$ regularization: A thresholding representation theory and a fast solver*, IEEE Trans. Neural Networks, 23 (2012), pp. 1013–1027.
- [44] P. YIN, E. ESSER, AND J. XIN, *Ratio and difference of l_1 and l_2 norms and sparse representation with coherent dictionaries*, Comm. Info. Systems, 14 (2014), pp. 87–109.

- [45] P. YIN, Y. LOU, Q. HE, AND J. XIN, *Minimization of ℓ_{1-2} for compressed sensing*, SIAM J. Sci. Comput., 37 (2015), pp. A536–A563.
- [46] S. ZHANG AND J. XIN, *Minimization of transformed l_1 penalty: Closed form representation and iterative thresholding algorithms*, Comm. Math. Sci., 15 (2017), pp. 511–537.
- [47] S. ZHANG AND J. XIN, *Minimization of transformed l_1 penalty: Theory, difference of convex function algorithm, and robust application in compressed sensing*, Math. Program., Ser. B, 169 (2018), pp. 307–336.
- [48] T. ZHANG, *Multi-stage convex relaxation for learning with sparse regularization*, in Adv. Neural. Inf. Process. Syst., 2009, pp. 1929–1936.
- [49] Y. ZHANG, *Theory of compressive sensing via $L1$ -minimization: a non-RIP analysis and extensions*, J. Oper. Res. Soc. China, 1 (2013), pp. 79–105.